FUSE

Far Ultraviolet Spectroscopic Explorer

Hot Molecular Hydrogen in M27 Observed by FUSE

Stephan R. McCandliss, Ken Sembach, Eric B. Burgh, & David J. Sahnow
Department of Physics and Astronomy, The Johns Hopkins University, 3400 N. Charles Street, Baltimore, MD 21218, stephan@pha.jhu.edu

Introduction: Hot and Cold H_2 Absorption Components

Recent *FUSE* observations of the very hot, $T_{eff} \sim 140{,}000$ K (Bohlin et al. 1982), central star of the planetary nebula M27 (NGC 6853, the Dumbbell) have revealed a far-UV spectrum unusually rich in molecular hydrogen absorption features (Figure 1 black line). We have identified two H_2 absorption systems separated by ≈ 42 km s^{-1}, with distinctly different ground state populations. The blueward component (RV $\approx$ -69 km s^{-1}) shows lines originating from a highly excited ground state, with rotational levels (J'') up to 15 and vibrational levels (v'') at least as high as 2. Many of the **lines absorbing out of $v'' = 1$ and 2** are located longward of the ground state bandhead ($v' - v'' = 0 - 0$) at 1108.12 Å, and **are unambiguous markers of hot H_2**. The redward component, at a RV ≈ -27 km s^{-1}, is "cool" ($J''_{max} \approx 5$, $v'' = 0$) and may be associated with foreground gas. However, the separation of the hot and cool components is within the range of velocity separations observed by Goudis et al. (1978) in Fabry-Perot interferograms of O I, N II and O III emission lines, so it is possible the cold component is associated with the nebula.

Synthetic Spectrum

A synthetic spectrum, shown in purple, is overplotted on the data in Figure 1. The stellar continuum is a Rauch (1998) model with T = 140k K, $\log g = 7$, d = 325 pc, and a far-UV extinction curve (E(B-V) = 0.05, $R_V = 3.2$ a little less steep than the galactic standard given in (Cardelli et al. 1989)), has been used to match the extincted continuum with the data. There is a two velocity component H_2 absorption model that assumes thermal equilibrium for the population of states with T = 200 K, b =2 km s^{-1}, $N^{cool}_{H_2} = 10^{18}$ cm^{-2}, for the cold component and T = 2400 K, b =5 km s^{-1}, $N^{hot}_{H_2} = 4.3 \times 10^{16}$ cm^{-2} for the hot. There is also a two velocity component H I absorption model with b = 10 km s^{-1}, $N_{HI} = 10^{20}$ cm^{-2} for each component.

Curve of Growth for the Hot H_2 Absorption

In Figure 2, a preliminary determination of the ground state ro-vibrational population distribution of the highly excited blueward component is shown. Equivalent widths of unblended lines (those with no overlapping hot or cold atomic and molecular components) were summed over a 0.16 Å region spanning the line center. Continuum determinations were made in a shoulder region to either side of the summation region and a straight line was fit through the mean of these points. Although this procedure is less accurate than can be achieved by hand it is simple and can be implemented automatically. However, there are systematics errors in the continuum placement. Nevertheless the large number of lines give us a level of statisical confidence in the temperature trend, the doppler parameter and the ortho-para modulation. We have less confidence in the individual ro-vibrational column densities.

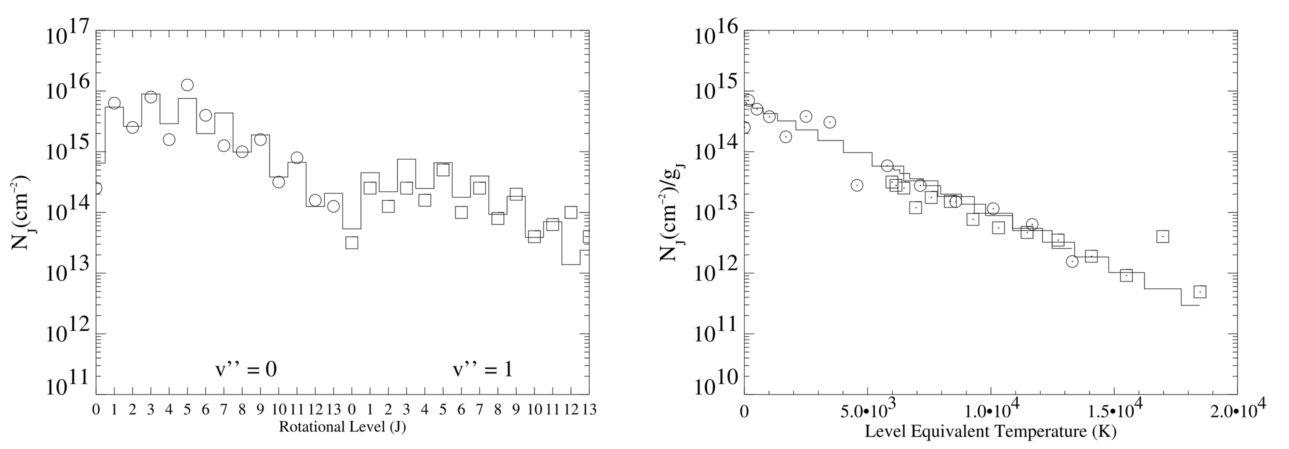

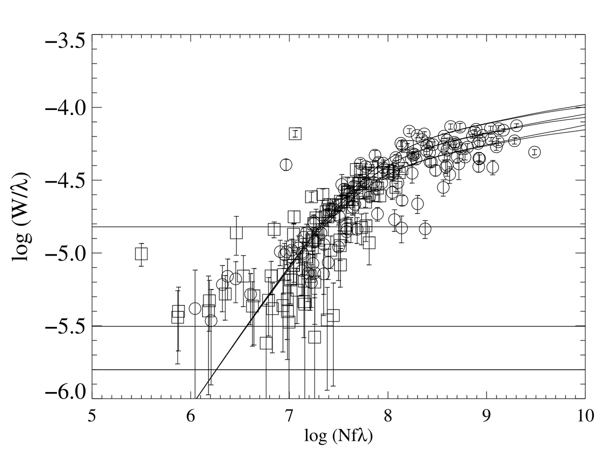

Fig. 2–In the upper left panel we show the curve-of-growth derived column densities as a function of ro-vibrational state quantum number, overplotted with a column density distribution computed for a temperature of 2400 K. In the upper right panel we show the column densities normalized by the level degeneracy for the same distributions, as a function of the level energy equivalent temperature. In the lower left panel we show curves-of-growth for doppler parameters of 3, 4 and 5 km s^{-1} along with the data. We note a doppler parameter of 4.45 km s^{-1} corresponds to a temperature of 2400 K. While there are significant deviations from the thermal population distribution the column densities follow the general trend of the 2400 K thermal population. There are a total of 222 lines on the curve-of-growth. We stress the preliminary nature of this work.

Shock or UV Fluorescent Excitation

M27 is a member of the class planetary nebula (PN) that follow "Gatley's rule," where infrared H_2 emission is a signature of bi-polar morphology (Zuckerman and Gatley 1988; Kastner et al. 1996). Zuckerman and Gatley (1988) concluded that the infrared H_2 emission is shock excited, based on IR spectroscopic diagnostics. This result is (perhaps) surprising because the presence of a hot star in such close proximity suggests that fluorescent excitation of H_2 might also be taking place. However, the Kastner et al. (1996) 2.122 μm image of M27 shows a patchy "bow tie" of emission with an outer radius $\sim 150''$, within which Zuckerman and Gatley (1988) have measured an average 2.122 μm brightness of 7.8×10^{-16} ergs cm^{-2} s^{-1} arcsec^{-2} . An integration of the unattenuated Rauch model over a 900 – 1100 Å bandpass shows only a modest UV intensity scale factor (for the average ISM background of Draine (1978)) at $150''$ of $\chi = 6$, which grows to $\chi = 100$ at $40''$. Following Sternberg (1989), we predict an average brightness per unit wavelength in the 900 – 1300 Å bandpass of $< 10^{-18}$ ergs cm^{-2} s^{-1} Å^{-1} arcsec^{-2} . In Figure 3 we show a recent longslit far-UV observation of M27 by JHU/NASA Sounding Rocket 36.136 UG. The extracted nebular spectrum on the right shows extended C II λ1335, C III λ1175, He II λ1085, possible H I two-photon emission, but no evidence for far-UV fluorenscent emission of H_2 to the background limit (shown in red) of $\approx 5 \times 10^{-17}$ ergs cm^{-2} s^{-1} Å^{-1} arcsec^{-2} ; a non-detection consistent with our far-UV fluorescence estimate. On the other hand if we use the Zuckerman and Gatley (1988) 2.122 μm brightness and assume all the infrared flux is caused by fluorescent excitation we would predict an average UV brightness per unit wavelength brightness of $\sim 2 \times 10^{-16}$ ergs cm^{-2} s^{-1} Å^{-1} arcsec^{-2} , which is comparable to the brightness of the detected emission features and would likely have been detected. **We conclude that shocks are the most likely cause for the excitation of the hot H_2.** We finally note that diffuse x-ray emission from M27 was detected by the ROSAT all sky survey, which Kreysing et al. (1992) have suggested might be caused by shock wave heating.

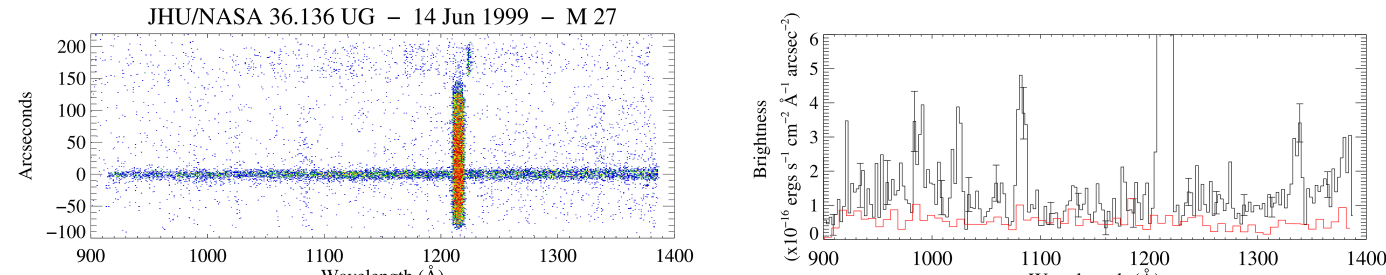

Fig. 3– Left panel is raw longslit far-UV spectrum. Right is the total nebular brightness per Å summed over the whole slit.

This work is based in part on data obtained for the Guaranteed Time Team by the NASA-CNES-CSA FUSE mission operated by the Johns Hopkins University supported by NASA contract NAS5-32985. Additional data has been obtained from a Johns Hopkins sounding rocket mission (36.136 UG) supported by NASA grant NAG5-5122.

Combined *FUSE* Spectrum of M27

Fig. 1—Here we show the spectrum of the CSPN, M27, produced from an 8 orbit concatenation of a time tagged photon list and a weighted average over the combined 8 spectral segments that comprise the *FUSE* spectrograph. The dispersion solutions for each segment are taken directly from the CALFUSE pipeline (v1.8.7). Wavelength co-alignment of the 8 segments was achieved thru a series of cross-correlations with LiF1ab serving as the scale fiducial. The position of geo-coronal Lyman–β defines the zeropoint. The data are shown in black and the lines are labeled; absorption lines from the top and emission lines from the bottom. The hot blueshifted H_2 components are labeled in blue, while the cool, less blueshifted, components are labeled in red. The length of the H_2 label tick is proportional to the line core optical depth (τ_c) of an assumed H_2 absorption model. Tick lengths that reach the bottom of the plot have $\tau_c \geq 1$. Lines with $\tau_c \leq 0.15$ have not been labeled. Emission lines have been labeled at the blueshift of the hot component, while atomic absorption lines have been labeled at the velocity shift of the cool component. The N I and N II lines are split and provide further evidence for the hot and cold dichotomy. The ratio of the N II hot and cool components line is about equal while the same ratio in the N I lines has a stronger the cool component. The radial velocity of the O VI λλ1032–1038 doublet (RV $\approx$ -40 km s^{-1}) is close to the systemic velocity found in Goudis et al. (1978) and Wilson (1953). These lines are relatively broad – compared to unblended H_2 lines – and we infer the doublet is photospheric in origin. If true they attest to the extreme temperature of the star. A two component synthetic spectrum, shown in purple, of the H I and H_2 absorption systems has been constructed and used to attenuate an extincted Rauch stellar model shown in orange. The extincted stellar model with H I absorption is in green.

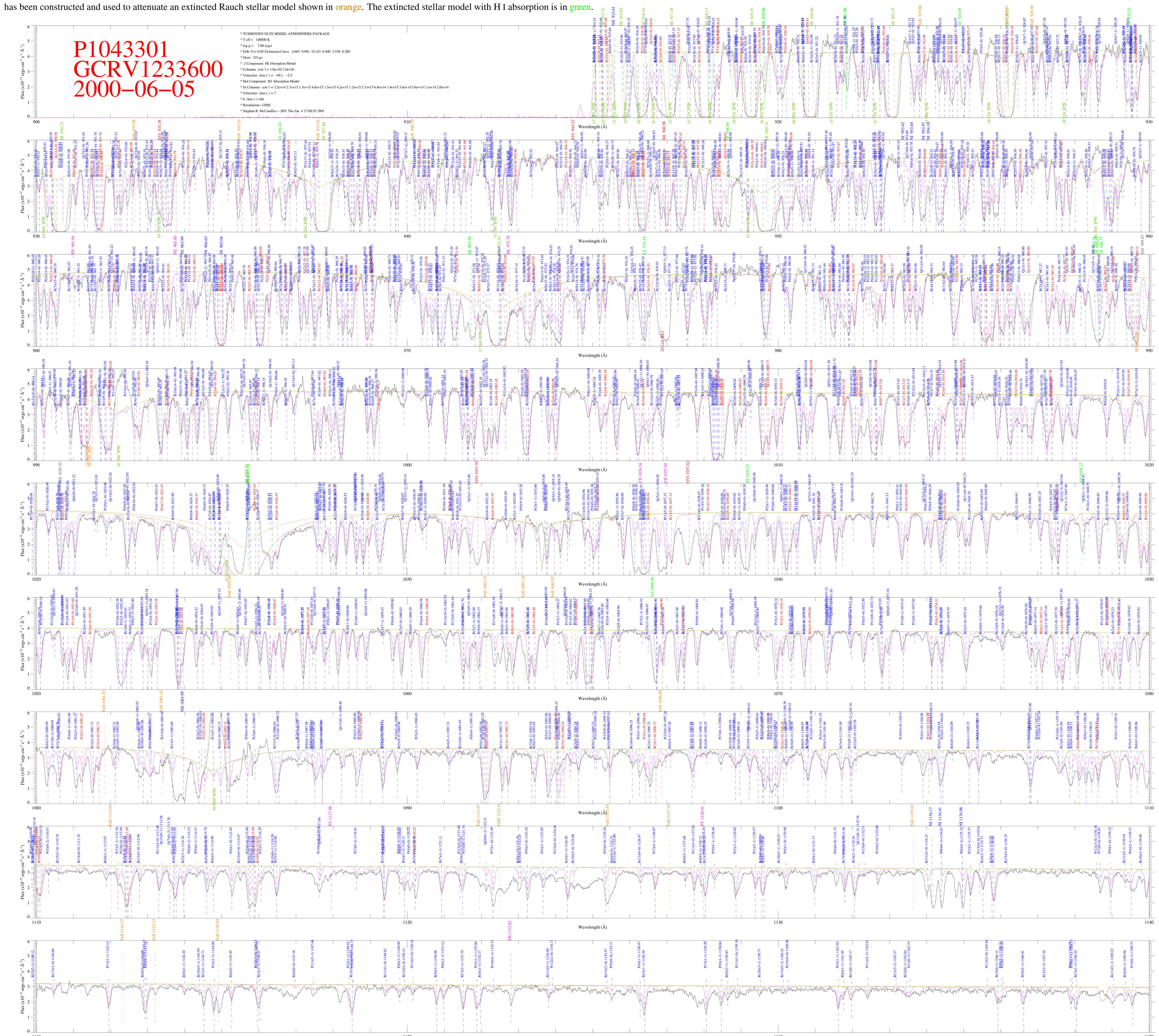

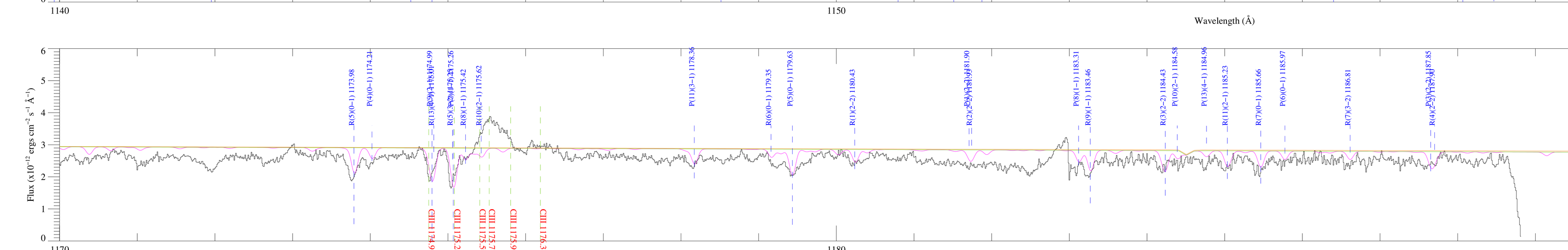

REFERENCES

Bohlin, R. C., Harrington, J. P., & Stecher, T. P. 1982, ApJ, 252, 635.
Cardelli, J. A., Clayton, G. C., & Mathis, J. S. 1989, ApJ, 345, 245.
Draine, B. T. 1978, ApJS, 36, 595.
Goudis, C., McMullan, D., Meaburn, J., Tebbutt, N. J., & Terrett, D. L. 1978, MNRAS, 182, 13.
Kastner, J. H., Weintraub, D. A., Gately, I., Merrill, K. M., & Probst, R. G. 1996, ApJ, 462, 777.
Kreysing, H. C., Diesch, C., Zweigle, J., Staubert, R., Grewing, M., & Hasinger, G. 1992, A&A, 264, 623.
Rauch, T. 1998. In *Ultraviolet Astrophysics Beyond the IUE Final Archive*, pp. 273+.
Sternberg, A. 1989, ApJ, 347, 863.
Wilson, R. E. 1953. In *Carnegie Institute Washington D.C. Publication*, pp. 0+.
Zuckerman, B., & Gatley, I. 1988, ApJ, 324, 501.

This poster (# 6.11) was prepared for Session 6. (Planetary Nebulae: Young and Old) at the *197th Meeting of the AAS* meeting in San Diego, CA, by Stephan McCandliss who corrupted Brian Wolven's (very nice) LaTeX Poster macros v2.1.

Fig. 1.—

Fig. 2.—

Fig. 3.—